JPCB Paper

DATASET · MARCH 2013

READS
111

4 AUTHORS, INCLUDING:

Murali Sankar Rajavelu
Central Leather Research Institute
19 PUBLICATIONS **184** CITATIONS
SEE PROFILE

Sellamuthu N Jaisankar
59 PUBLICATIONS **291** CITATIONS
SEE PROFILE

Asit Baran Mandal
Central Leather Research Institute
360 PUBLICATIONS **3,202** CITATIONS
SEE PROFILE

THE JOURNAL OF PHYSICAL CHEMISTRY B

Article

pubs.acs.org/JPCB

Physicochemical Studies on Polyurethane/Siloxane Cross-Linked Films for Hydrophobic Surfaces by the Sol–Gel Process

Kamal Mohamed Seeni Meera,[†] Rajavelu Murali Sankar,[†] Sellamuthu N. Jaisankar,[†] and Asit Baran Mandal*[,†,‡]

[†]Polymer Division, Council of Scientific and Industrial Research (CSIR) – Central Leather Research Institute (CLRI), Adyar, Chennai 600020, Tamil Nadu, India

[‡]Chemical Laboratory, Council of Scientific and Industrial Research (CSIR) – Central Leather Research Institute (CLRI), Adyar, Chennai 600020, Tamil Nadu, India

S *Supporting Information*

ABSTRACT: A series of castor oil based polyurethane/siloxane cross-linked films were prepared using castor oil, isophorone diisocyanate, and 3-aminopropyl trimethoxysilane by the sol–gel process. Fourier transform infrared (FT-IR) spectra reveal the cross-linking interaction between polyurethane and siloxane moieties, thereby shifting the peak position of characteristic N—H and C═O groups to higher wavenumber. ^{29}Si (silica) solid state nuclear magnetic resonance spectra were used to prove the formation of siloxane network linkage in the polyurethane system, thereby analyzing the Si environment present in the polyurethane/siloxane cross-linked films. The activation energy values at two stages (T_{max1} and T_{max2}) for the degradation of polyurethane films were increased with increasing silane ratio. The calculated activation energy values for the higher silane ratio (1.5) are 136 and 170 kJ/mol at T_{max1} and T_{max2}, respectively. From contact angle measurements, we observed that increasing siloxane cross-linking increased the hydrophobicity of the films. The optical transmittance obtained from ultraviolet–visible spectra indicated that the film samples are transparent in the region 300–800 nm. The moisture sorption/desorption isotherm curve shows a characteristic behavior of type III isotherm corresponds to hydrophobic materials. Dynamic mechanical studies show that the increase in storage modulus reveals siloxane cross-linking gives rigidity to the films. Atomic force microscopic images show that the introduction of siloxane changes the surface roughness of the polyurethane films. It is found that the siloxane cross-linking can be used to obtain hydrophobic surface films having good thermal stability and optical transmittance.

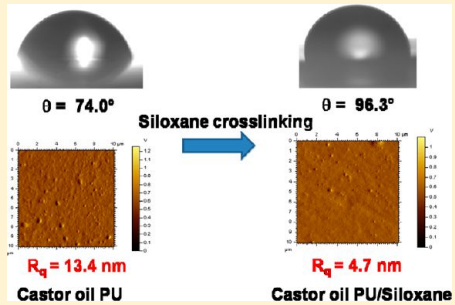

1. INTRODUCTION

In recent years, the polymeric materials based on renewable resources like vegetable oils have attracted much attention due to their ready availability and versatile applications.[1] Among them, castor oil (CO) based polyurethane (PU) is the most important one. Castor oil is an important vegetable oil containing hydroxyl groups, which are used to obtain oil based polyurethane.[2,3] The vegetable oil based polyurethanes have the following advantages: high strength, stiffness, environmental resistance, and long life properties.[4] Castor oil replaced polyol from petrochemicals owing to its stability at different temperatures and pressures.[5] These polyurethanes show good miscibility with natural polymers to give semi-interpenetrating networks. Due to its elasticity and flexibility, these polyurethanes were used as individual polymer processing network structures.[6,7] Polyurethanes are widely used in coatings,[8] wound dressings, shape memory applications, rubber, textiles,[9] leather, adhesives, liquid crystals,[10] and nanobiomaterials.[11] Oil based polymers are important for biomedical applications due to their excellent mechanical, high biocompatibility, and high flexural endurance properties.[12] The use of renewable sources like vegetable oils in polyurethane synthesis might be realized in environmental protection.[13] Castor oil based elastomeric polyurethanes were used for the fabrication of microfluidic devices by rapid prototyping.[14]

Over the years, there has been growing interest in the area of preparing organic–inorganic hybrid nanocomposites due to their improved thermal, mechanical, and biological properties.[15,16] The widely used method to introduce an inorganic system (silica) into the polymeric matrix is a sol–gel approach.[17−19] The major advantage of using a sol–gel method is the mild reaction conditions like low temperature used to prepare silica (Si) nanoparticles.[20] Silicate is the common species found in the Earth's crust and mantle.[21] There is a drawback that the silica formation does not have a good compatibility with polymer matrix.[22] In order to overcome this drawback, cross-linking agents were used. 3-Aminopropyl trimethoxysilane (APTMS) is one of the cross-linkers used to produce cross-linked polyurethane structures, in which a methoxy group undergoes a cross-linking reaction to form

Received: October 1, 2012
Revised: February 2, 2013
Published: February 11, 2013

   dx.doi.org/10.1021/jp3097346 | *J. Phys. Chem. B* 2013, 117, 2682–2694

stable siloxane network structures with a silylated polyurethane moiety.[23] Recently, Arunbabu et al.[24] reported poly(acrylic acid-*co*-*N*,*N*′-methylenebisacrylamide) hydrogel films by using the copolymerization method using acrylic acid with *N*,*N*′-methylenebisacrylamide as a cross-linker via the photopolymerization technique.

The introduction of a siloxane unit in the polyurethane received much attention due to its several advantages including good thermal stability and high flexibility at low temperature.[25] Often polyurethane−siloxane systems are formed as a cross-linkable matrix. Polyurethane−siloxane structures may have excellent mechanical properties over conventional polyurethanes and biostability of silicon rubber.[26] A siloxane unit (Si−O−Si) was formed through a sol−gel hydrolysis and condensation of an alkoxy group.[27] These kinds of polymer−silica materials have promising applications in the medicinal field, as they have good compatibility with living matters.[28] Siloxane−carbonate based polyurethanes were reported to have wide potential applications in the cardiac and orthopedic biomedical fields.[29] Siloxane cross-linked polyurethane elastomers were reported to have an inflammatory response with a short degradation time.[30] Ni et al.[31] have reported polyurethane/polysiloxane based ceramic coatings for the evaluation of corrosion protection. Siloxane−polyurethane cross-linked coatings were widely used in fouling-release marine coatings.[32,33] Poly(*N*-vinylpyrrolidone) modified poly(dimethylsiloxane) elastomeric surfaces may be useful in the applications of antibiofouling surfaces.[34]

In the present work, we prepared a series of castor oil based polyurethane/siloxane cross-linked structures as films through a sol−gel process, which was not reported to the best of our knowledge. Therefore, the influence of siloxane cross-linking on the structural, thermal, and mechanical properties of the above polyurethane films were studied using several techniques, viz., attenuated total reflectance-Fourier transform infrared (ATR-FTIR) spectroscopy, solution nuclear magnetic resonance (NMR) spectroscopy, ^{29}Si solid state cross-polarization magic-angle-spinning (CP/MAS) NMR spectroscopy, thermogravimetric analysis (TGA), differential scanning calorimetry (DSC), contact angle measurement for surface energy determination, ultraviolet−visible (UV−vis) studies, moisture sorption analysis for water sorption capacity, dynamic mechanical analysis (DMA), scanning electron microscopy-energy dispersive X-ray (SEM-EDX), and atomic force microscopy (AFM) with a view to stimulate the results in physical chemistry standpoints.

2. EXPERIMENTAL SECTION

2.1. Materials and Methods. Agmark grade castor oil (Molecular formula: $C_{57}H_{104}O_9$, hydroxyl number: 164 mg KOH/g, mol wt: 932) was purchased from Bison Laboratories, India. Castor oil was heated at 80 °C for 4 h to remove the moisture. Isophorone diisocyanate (IPDI), 3-aminopropyl trimethoxysilane, and chloroform-d_6 ($CDCl_3$) were purchased from Aldrich, USA. Dibutyltin dilaurate (DBTDL) catalyst was obtained from Fluka, USA. Chloroform was purchased from Merck Laboratories, India, and distilled before use. All the reagents were used as received.

2.2. Preparation of Castor Oil Polyurethane/Siloxane Cross-Linked Structure. Scheme 1 shows the preparation of castor oil polyurethane/siloxane cross-linked structures. The above compounds with cross-linked structures were synthesized in a three-necked round-bottom flask equipped with a magnetic stirrer, a nitrogen (N_2) inlet, and an addition funnel for adding diisocyanate and solvent. A calculated amount of castor oil (2.796 g) was taken in a 100 mL round-bottom flask and then heated to 70 °C and dissolved in 10 mL of chloroform. Then, the required amount of isophorone diisocyanate was added dropwise to it with continuous stirring. The NCO:OH ratio used here is 3:1. After that, 0.001% of dibutyltin dilaurate catalyst was introduced into the system and the reaction continued for 4 h at 70 °C under N_2 atmosphere. The castor oil polyurethane prepolymer was obtained at the end of 4 h. After 4 h, the required amount of 3-aminopropyl trimethoxysilane was added dropwise to it. Then, the reaction further continued

Scheme 1. Preparation of Castor Oil Polyurethane/Siloxane Cross-Linked Structures

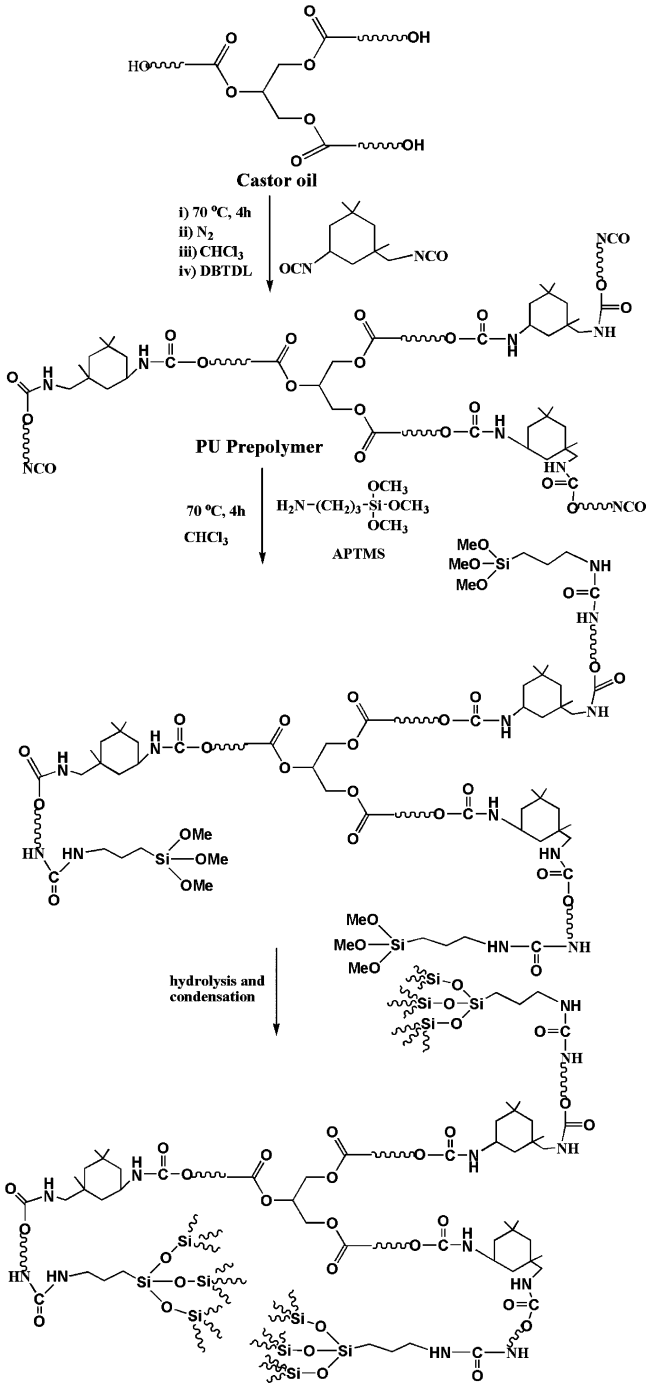

dx.doi.org/10.1021/jp3097346 | J. Phys. Chem. B 2013, 117, 2682−2694

for another 4 h at 70 °C. The chloroform level was maintained to avoid the gel formation throughout the reaction. After 8 h, the reaction mixture was casted in a Petri-dish to obtain it as a film. The sample codes and compositions of films were given in Table 1.

Table 1. Codes and Compositions of the Polyurethane/Siloxane Cross-Linked Structure Films

	compositions		
codes	CO (g)	NCO:OH ratio	APTMS ratio
PU 0.0			0.0
PU 1.0			1.0
PU 1.1			1.1
PU 1.2	2.796	3:1	1.2
PU 1.3			1.3
PU 1.4			1.4
PU 1.5			1.5

2.3. Characterization. The infrared spectra of the polyurethane/siloxane film samples were recorded on an ABB MB3000 Fourier-transform infrared spectrometer in ATR mode over 60 scans with a resolution of 16 cm^{-1} over a zinc selenide surface. Solution ^{1}H NMR spectroscopic analysis was recorded in $CDCl_3$ using a JEOL ECA 500 MHz high resolution NMR spectrometer. ^{29}Si solid state NMR spectra were recorded using a Bruker Avance 400 spectrometer, Germany, at a frequency of 79.49 MHz for ^{29}Si cross-polarization magic-angle-spinning (CP/MAS) NMR with reference to tetramethylsilane (TMS). The relaxation delay between pulses is 5.0 s with 3.5 ms contact time. The spectra were recorded over a 5000 scans along with a spectral width of 604.8 ppm. The chemical shifts taken in the spectra of silicate range from −250 to 250 ppm. Thermogravimetric analyses were done using a TG Analyzer-Model Q50, TA Instruments, from 30 to 800 °C under N_2 atmosphere with a flow rate of 40−60 mL/min with different heating rates of 5, 10, 15, and 20 °C/min. Differential scanning calorimetric analyses were performed using a DSC-Model Q200, TA Instruments, by heating the samples from −90 to 300 °C at a heating rate of 10 °C/min with a N_2 flow of 50 mL/min. The static contact angles were measured on a contact angle meter from Holmarc Opto Mechatronics Pvt Ltd., India. The static contact angle of water and hexadecane (volume of 5 μL) were measured, and the surface free energy was calculated using the Owens and Wendt equation. The contact angle values reported are averages of five measurements taken at five different locations of the film surface (see Table S1 and Figure S1, Supporting Information). UV−vis transmittance spectra were recorded on a Shimadzu UV-2401 spectrophotometer. Moisture sorption analysis was carried out using a moisture sorption analyzer (Q 5000 SA, TA Instruments, USA) under controlled conditions of temperature and relative humidity (RH). The stepwise adsorption and desorption studies of the film samples were carried out from 0% RH to 90% RH and back at a step interval of 10% RH at 25 °C. At each RH level, equilibration was stopped when the relative change in sample mass remained below 0.01% for 5 min, and the next RH step was automatically applied. DMA was done using a Metravib dynamic mechanical analyzer system 50 N with multifrequencies (0.1, 0.5, 1, 2, and 5 Hz) at two different temperatures −100 and 100 °C. Scanning electron microscopy (SEM) and energy dispersive X-ray (EDX) spectrometry of the film samples were done using a Quanta 200 FEG scanning electron microscope in low vacuum mode operating at 20 kV. AFM measurements were conducted using an Agilent Technologies 5500 scanning probe microscope, USA, in tapping mode. AFM analysis was done on the surface of the film with a scanning area of 10 μm × 10 μm.

3. RESULTS AND DISCUSSION

Figure 1 shows the ATR-FTIR spectra for the prepared polyurethane/siloxane films. In Figure 1a, the characteristic

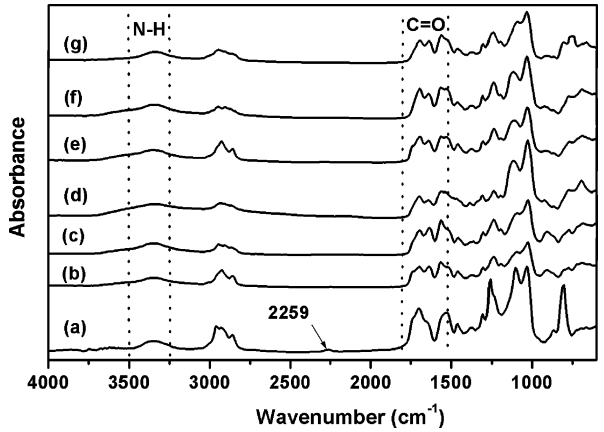

Figure 1. ATR-FTIR spectra for the polyurethane/siloxane films: (a) PU 0.0, (b) PU 1.0, (c) PU 1.1, (d) PU 1.2, (e) PU 1.3, (f) PU 1.4, and (g) PU 1.5.

Table 2. Characteristics of N—H and C═O Regions in the IR Spectra of PU 1.0 Sample at Different Time Intervals during the Second Stage of the Reaction

time (min)	N—H region (cm^{-1})	urethane C═O region (cm^{-1})	urea C═O region (cm^{-1})	Si—O vibration (cm^{-1})
0	3336.1	1712.3		
270	3337.4	1722.1	1632.3	1057.3
300	3341.2	1724.4	1634.2	1058.2
360	3342.1	1726.5	1636.1	1064.0
420	3342.5	1728.1	1637.0	1088.0
480	3344.0	1742.0	1638.0	1094.2

peaks, viz., C═O, N—H vibration, and free NCO in urethane appear at 1739, 3342, and 2259 cm^{-1}, respectively. In Figure 1b−g, the free NCO peak was completely disappeared, which indicated that all the NCO groups were reacted with the amino group of APTMS. The peaks appearing in the range 2857−2925 cm^{-1} correspond to the —CH_2 stretching vibration of the alkyl chain present in castor oil. The formation of the silylated polyurethane moiety was confirmed from the appearance of the urea C═O peak at 1637 cm^{-1}.[35] The peak observed at around 772 cm^{-1} confirms the presence of the O—Si—O stretching vibration.[36] The appearance of the peak at 1094 cm^{-1} implies characteristic Si—O stretching vibration, which proves the formation of a siloxane linkage.

The urethane N—H region of PU 0.0 appears at 3342 cm^{-1}, whereas, in the case of siloxane cross-linked films, they show the N—H peak at 3358 cm^{-1} (PU 1.3) with an increase in intensity. This may be due to the overlapping of the urethane and urea N—H peaks. The N—H peak position shifts to higher wavenumber with increasing silane ratio (3342, 3344, and 3358 cm^{-1} for PU 0.0, PU 1.0, and PU 1.3, respectively).

dx.doi.org/10.1021/jp3097346 | J. Phys. Chem. B 2013, 117, 2682−2694

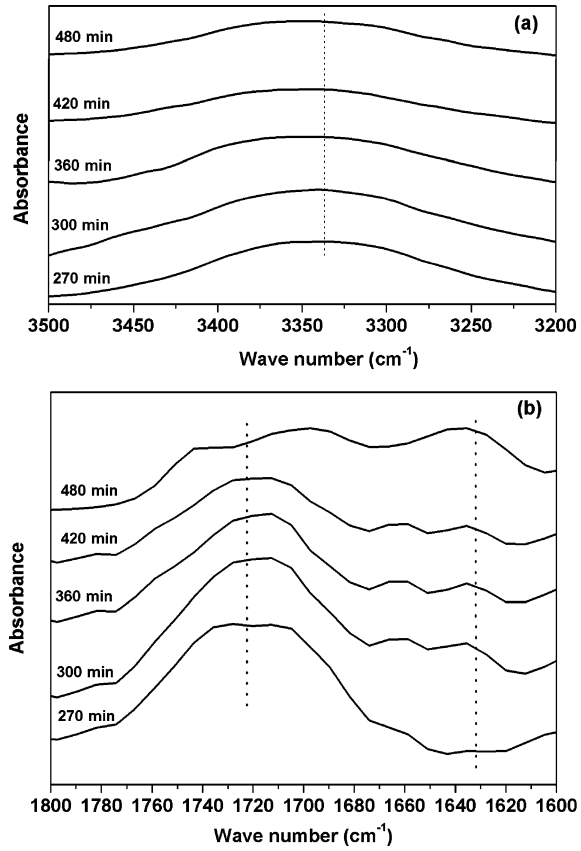

Figure 2. ATR-FTIR spectra for the expanded regions of PU 1.0 at different time intervals: (a) N—H region (3500–3300 cm^{-1}) and (b) C═O region (1800–1600 cm^{-1}).

This may be due to the cross-linking behavior among the N—H groups in polyurethane/siloxane films. Similarly, the C═O group gives two peaks corresponding to the urethane and urea regions of the polyurethane moiety. The peak appeared at around 1739 cm^{-1} due to the urethane C═O group, and the peak at around 1637 cm^{-1} was assigned to the urea C═O group. The peak position of urethane C═O shifts to a higher wavenumber from 1739 (PU 0.0) to 1742 and 1745 cm^{-1} for PU 1.0 and PU 1.3, respectively. Similarly, the peak position of urea C═O also shifted toward higher wavenumber. The peak values for C═O of urea are 1637 (PU 0.0), 1638 (PU 1.0), 1640 (PU 1.2), and 1641 cm^{-1} (PU 1.3). It is observed that a strong cross-linking interaction occurred in the polyurethane/siloxane films.

Furthermore, to understand the effect of reaction time on the FT-IR peaks of the N—H and C═O regions of polyurethane/siloxane film, we presented the time-dependent peak shifts for the polyurethane/siloxane film (PU 1.0) during the siloxane formation stage. The formation of siloxane increases the cross-linking, which resulted in the shift of the peaks to higher wavenumber. In the case of the N—H region, the peak position was shifted from 3336.1 (at the start of the reaction, 0 min) to 3344.0 cm^{-1} (at the end of the reaction, 480 min). The FT-IR data (Table 2) and the spectra (Figure 2) were presented for the second stage of the reaction (after the addition of APTMS). The shift in the wavenumber for the N—H region was around 6 cm^{-1} with increased intensity (Table 2). The area of the peak at the end of the reaction becomes much broader (Figure 2a). This indicates that the increase in cross-linking provides a substantial increase in interaction among the N—H groups in polyurethane/siloxane film.[7] Similarly, the C═O region of the urethane and urea groups gives shifting of the peaks to a higher wavenumber (Figure 2b). This proves that the increasing reaction time provides the evidence of the cross-linked state of the polyurethane/siloxane films, thereby shifting the peak position of the corresponding N—H and C═O groups. On the other hand, the Si—O stretching vibration was also monitored during the course of the reaction at different time intervals. At the start of the reaction (270 min), the peak appeared at around 1057 cm^{-1}. Over a period of reaction time, there is a substantial increment in the peak position of Si–O vibration (Table 2).[34] At the end of the reaction (480 min), the peak position was shifted to 1094 cm^{-1}, which clearly shows the increment in the number of siloxane groups. This increment results in more cross-linked structure in the polyurethane/siloxane films. Overall, this indicates that there is a strong interaction between the polyurethane and siloxane groups.

The solution ^{1}H NMR spectra were recorded to confirm the formation of castor oil based polyurethane/siloxane structure and depicted in Figure 3. The ^{1}H NMR spectrum for the native castor oil[37,38] (Figure 3a) gives a multiplet at 4.06–4.28 ppm that corresponds to —CH_2 groups of glycerol, a multiplet at 5.18–5.24 ppm because of the —CH group present in the glycerol moiety, CH_2 attached to ester —C—O appeared as a triplet at 2.23–2.29 ppm, the CH_2 chain appeared at 1.35–1.63 ppm, CH_2 attached to C═C on the aliphatic side appeared at 1.96–2.04 ppm, CH_2 attached to C═C on the side of —OH appeared at 2.13–2.19 ppm, the multiplet at 3.51–3.60 ppm corresponds to C—H attached to OH, terminal aliphatic CH_3 groups appeared at 0.80–0.87 ppm, and a multiplet appeared at 5.26–5.53 ppm belonging to a —CH═CH— group.[39] In the ^{1}H NMR spectrum of castor oil polyurethane/siloxane (Figure 3b), new peaks appeared along with the characteristic castor oil peaks. The urethane N—H proton appeared at around 7.08–7.12 ppm, whereas the urea N—H proton appeared at 5.89 ppm. In the case of the ^{1}H NMR spectrum of castor oil prepolymer (without addition of APTMS), only the urethane N—H proton appeared at 7.0–7.05 ppm (data not shown). This proves the formation of urea in the second stage of the reaction (after the addition of APTMS). Further, a new peak appeared at 3.06 ppm, which corresponds to —CH_2 adjacent to urea N—H.[40] The C—H attached with urethane N—H showed a downfield shift than native castor oil (4.60–4.76 ppm), which evidences the formation of a urethane linkage. The appearance of two peaks at 1.39 and 1.52 ppm assigned to methylene protons of APTMS. A broad peak at 5.0 ppm shows the presence of a Si—OH group in the final product.

The ^{29}Si environment present in the polyurethane/siloxane films was also characterized by ^{29}Si solid state CP/MAS NMR spectroscopy, and the spectra were given in Figure 4. ^{29}Si solid state CP/MAS NMR chemical shift values for the Q and T environments present in polyurethane/siloxane films were presented in Table 3. Siloxane network structures present in the polyurethane/siloxane cross-linked films were identified using ^{29}Si NMR. In cross-linked films, silicon atoms are present as mono-, di-, tri-, and tetra- substituted siloxane linkages and the bonds are designated as Q^1 (mono-), Q^2 (di-), Q^3 (tri-), and Q^4 (tetra-), respectively. The sample PU 1.0 shows the chemical shift values of Q^1, Q^2, and Q^3 are −92.8, −95.5, and −96.7 ppm which shows the presence of mono-, di-, and tri-substituted siloxane bonds and for T^3 is −78.8 ppm (i.e., nonhydrolyzed species present in PU 1.0) (Figure 4a).[41,42] In the case of PU 1.1 (Figure 4b), only Q^2 and Q^3 environments were present at

dx.doi.org/10.1021/jp3097346 | J. Phys. Chem. B 2013, 117, 2682–2694

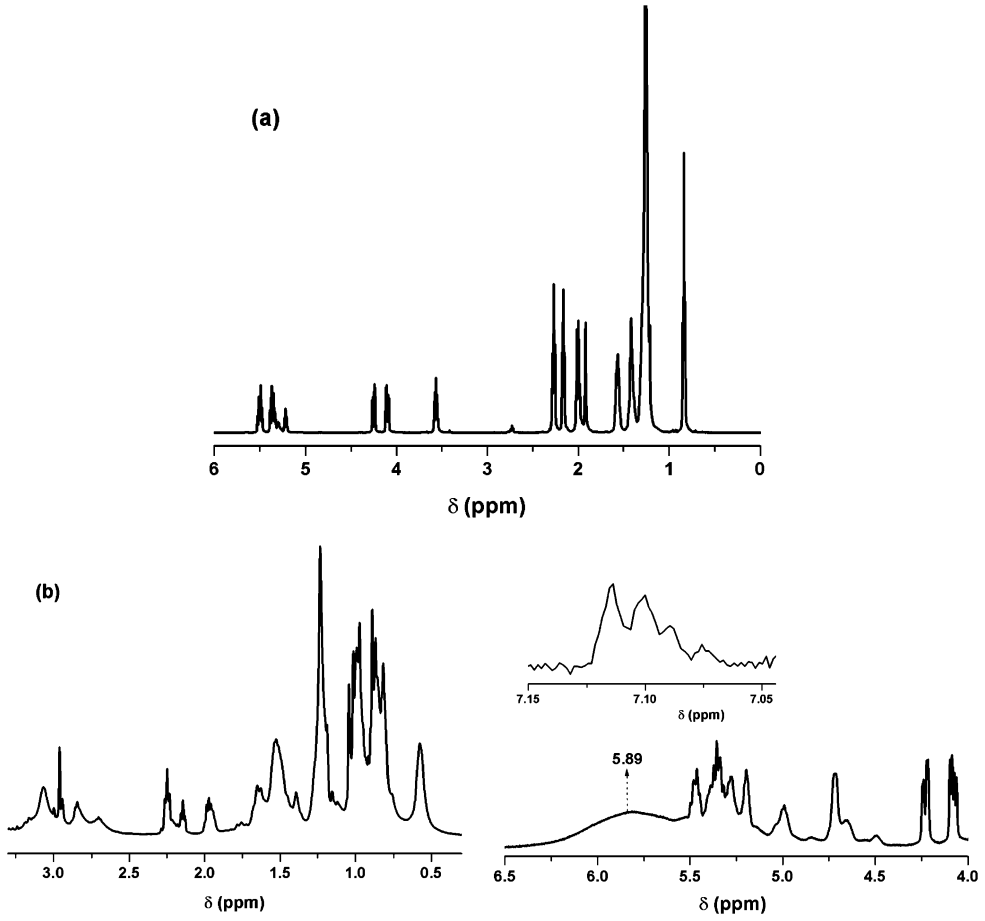

Figure 3. Solution ^{1}H NMR spectra of (a) castor oil and (b) polyurethane/siloxane structure.

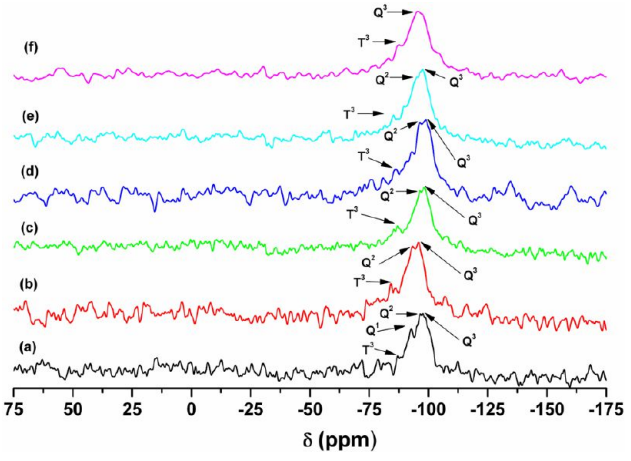

Figure 4. ^{29}Si solid-state CP/MAS NMR spectra of polyurethane/siloxane structure films: (a) PU 1.0, (b) PU 1.1, (c) PU 1.2, (d) PU 1.3, (e) PU 1.4, and (f) PU 1.5.

−93.5 and −96.0 ppm including T^3 at −78.3 ppm. This shows that increasing silane concentration results in more siloxane bonds with a similar environment, which results in further cross-linking. Moreover, increasing the silane mole ratio from 1.0 to 1.5, the spectrum gives a single broad peak corresponding to the Q^3 structure at −98.7 ppm (Figure 4f), which confirms the formation of trisubstituted siloxane bonds.[43] Also, the T^3 peak appeared at around −82.4 ppm. This proves the formation of network structure from major

Table 3. ^{29}Si Solid State CP/MAS NMR Chemical Shift Values for the Q and T Environments Present in Polyurethane/Siloxane Films

	chemical shift values (ppm)			
codes	Q^1	Q^2	Q^3	T^3
PU 1.0	−92.8	−95.5	−96.7	−78.8
PU 1.1		−93.5	−96.0	−78.3
PU 1.2		−95.3	−97.4	−76.3
PU 1.3		−96.2	−97.7	−79.9
PU 1.4		−95.2	−97.7	−79.9
PU 1.5			−98.7	−82.4

microstructures Q^1, Q^2, Q^3, and T^3. It was observed that the dominance of the Q^3 peak (Figure 4f) in the higher silane content (PU 1.5) demonstrates a higher degree of inorganic condensation (i.e., cross-linking) occurred in the polyurethane/siloxane system.[44] The ^{29}Si solid state CP/MAS NMR proves the formation of a siloxane linkage network structure in the polyurethane system.

TGA of the polyurethane/siloxane films at different heating rates is depicted in Figure 5. The weight loss up to 200 °C is due to the evaporation of residual moisture present in the films. The weight loss in the range 250−350 °C is attributed to the dissociation of urethane bonds to form isocyanates, alcohol, amines, and CO_2.[45] The degradation above 400 °C is mainly due to the scission of the castor oil chain. The major decomposition products are 10-undecanoic acid and heptanol.[46] All the film samples show two-stage decomposition

dx.doi.org/10.1021/jp3097346 | J. Phys. Chem. B 2013, 117, 2682−2694

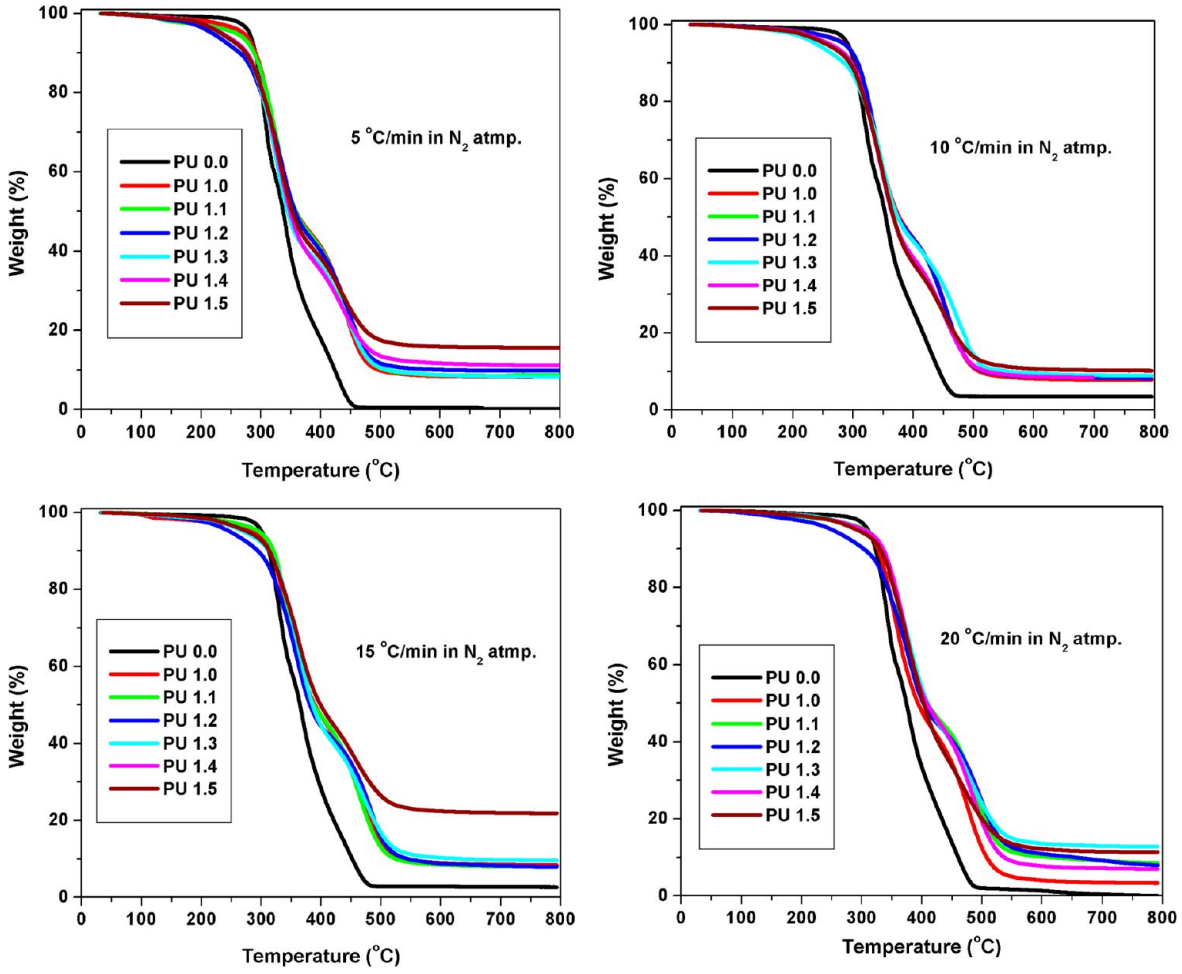

Figure 5. TGA thermograms for the castor oil polyurethane/siloxane films at different heating rates.

Table 4. Thermogravimetric Data for the Castor Oil Polyurethane/Siloxane Films

	first stage degradation temperature T_{max1} (°C) at different heating rates (°C/min)				second stage degradation temperature T_{max2} (°C) at different heating rates (°C/min)			
codes	5	10	15	20	5	10	15	20
PU 0.0	306	320	330	343	343	356	368	379
PU 1.0	319	336	346	356	438	450	468	479
PU 1.1	330	337	351	366	439	454	470	487
PU 1.2	337	345	355	374	449	465	487	497
PU 1.3	340	352	361	376	450	468	466	481
PU 1.4	341	354	360	373	446	467	471	485
PU 1.5	345	355	364	377	438	454	460	475

temperatures (Figure 5). The onset of degradation temperature of cross-linked films was increased with increasing silane ratio (Table 4). The first-stage degradation temperature (T_{max1}) value increased with increasing heating rate of the degradation process. However, the second-stage degradation temperature (T_{max2}) value shows slight deviation with increasing heating rate of the degradation process. It is important to note that the T_{max2} values were increased with respect to the heating rates until the silane ratio of 1.2 (PU 1.2), and after that the T_{max2} value decreased. The weight loss behavior of polyurethane/siloxane films at 350 and 450 °C was given in Table 5 at different heating rates. Overall, the presence of higher siloxane content increases the cross-linking, which yields a higher degradation temperature.

Table 5. Weight Loss Behavior for the Castor Oil Polyurethane/Siloxane Films

	% decomposition up to 350 °C at different heating rates (°C/min)				% decomposition up to 450 °C at different heating rates (°C/min)			
codes	5	10	15	20	5	10	15	20
PU 0.0	62.36	48.78	41.23	37.08	96.85	96.02	89.25	89.75
PU 1.0	46.87	37.59	30.86	24.11	79.47	71.37	66.15	65.43
PU 1.1	47.58	38.31	29.49	17.86	78.32	71.80	66.84	58.22
PU 1.2	47.01	37.63	31.69	23.44	76.48	67.55	64.88	59.54
PU 1.3	52.98	39.82	27.34	17.50	78.70	74.78	66.89	60.27
PU 1.4	50.90	39.25	26.37	16.51	78.22	74.67	62.02	60.14
PU 1.5	37.97	36.95	25.32	15.60	69.82	68.28	60.31	56.24

dx.doi.org/10.1021/jp3097346 | J. Phys. Chem. B 2013, 117, 2682−2694

Table 6. Calculated Activation Energies of Castor Oil Polyurethane/Siloxane Films

	first stage degradation, T_{max1}			second stage degradation, T_{max2}		
codes	slope	E_a (kJ/mol)	correlation coefficient (R^2)	slope	E_a (kJ/mol)	correlation coefficient (R^2)
PU 0.0	−12289	102	0.9694	−13584	113	0.9658
PU 1.0	−12685	105	0.9989	−14186	117	0.9096
PU 1.1	−13540	113	0.9123	−15501	128	0.9755
PU 1.2	−14343	119	0.9072	−16271	135	0.9429
PU 1.3	−14782	122	0.9471	−18047	150	0.9639
PU 1.4	−15313	127	0.9947	−18422	153	0.9759
PU 1.5	−16309	136	0.9278	−20488	170	0.9070

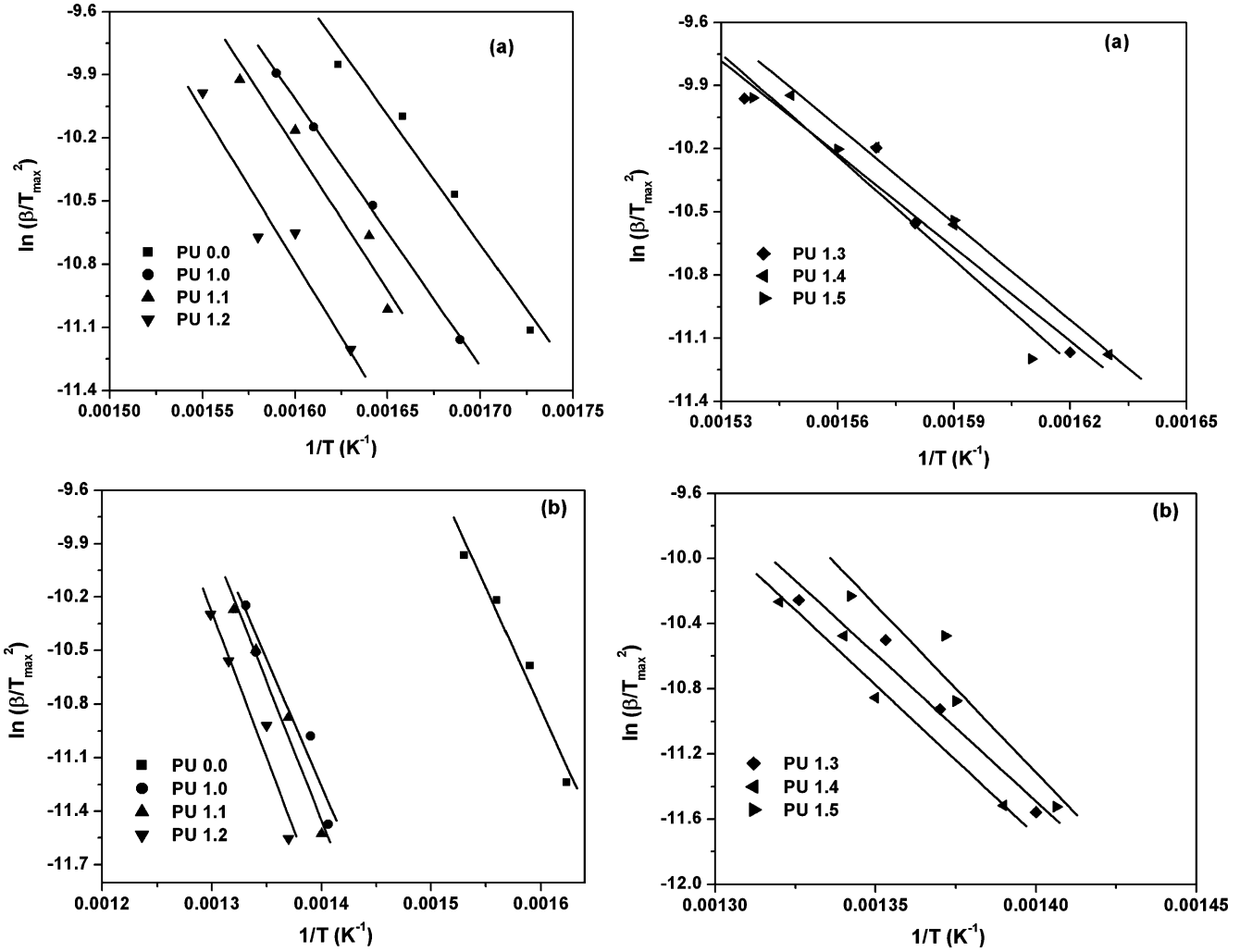

Figure 6. Kissinger plots for the polyurethane/siloxane films at two different stages: (a) T_{max1} and (b) T_{max2}.

The activation energy for the decomposition process of castor oil polyurethane/siloxane film samples was calculated by the Kissinger method using the following equation:[47−49]

$$\ln\left(\frac{\beta}{T_{max}^{2}}\right) = -\frac{E_a}{RT_{max}} + \left\{\ln\frac{AR}{E_a} + \ln[n(1-\alpha_{max})^{n-1}]\right\} \quad (1)$$

where β = heating rate, T_{max} = temperature corresponding to the maximum degradation, A = pre-exponential factor, E_a = activation energy, α_{max} = maximum conversion, n = order of the reaction, and R is the universal gas constant. A plot of $\ln(\beta/T_{max}^2)$ versus $1/T_{max}$ should give a straight line with the slope being $-E_a/R$.

The calculated activation energies (E_a) for the castor oil polyurethane/siloxane films were given in Table 6, and the Kissinger plots at two different degradation stages were shown in Figure 6. The activation energy values were increased with increasing silane ratio, which shows that the thermal stability of the system increased with increasing cross-linking. The activation energy (E_a) for the control polyurethane (PU 0.0) system is 102 and 113 kJ/mol at T_{max1} and T_{max2}, respectively. However, in the case of PU 1.5, the E_a values are 136 and 170 kJ/mol at T_{max1} and T_{max2}, respectively. The higher the cross-linking, the higher thermal stability of the film that was obtained (see Table 6). The incorporation of a siloxane unit in

dx.doi.org/10.1021/jp3097346 | J. Phys. Chem. B 2013, 117, 2682−2694

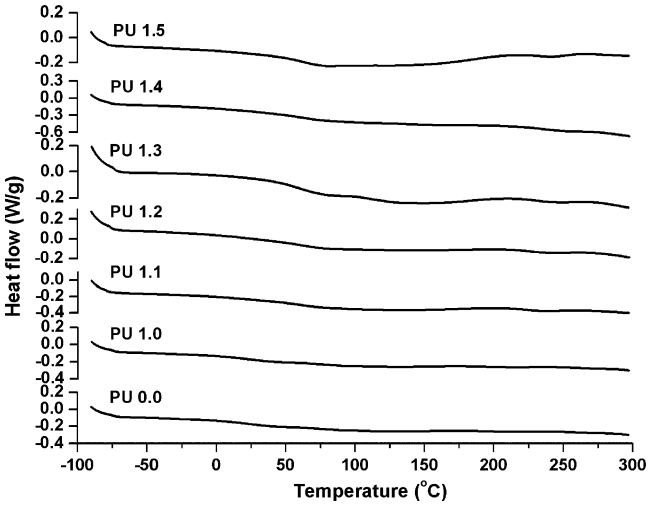

Figure 7. DSC of polyurethane/siloxane films.

Table 7. DSC Data of the Polyurethane/Siloxane Cross-Linked Structure Films

	thermal properties		
codes	T_g (°C)	T_m (°C)	ΔH (J/g) for T_m
PU 0.0	−33.3	209.6	1.5
PU 1.0	−28.7	234.5	2.4
PU 1.1	−30.7	237.8	2.7
PU 1.2	−29.2	243.3	3.1
PU 1.3	−32.5	247.9	2.2
PU 1.4	−30.5	242.9	2.7
PU 1.5	−27.5	258.6	2.8

Table 8. Contact Angle and Surface Free Energy Values for the Polyurethane/Siloxane Films

	static contact angle (deg)		surface free energy (mJ/m^2)		
codes	water	hexadecane	γ_s^p	γ_s^d	γ_s^t
PU 0.0	74.0	8.9	9.2	28.4	37.6
PU 1.0	79.7	7.3	6.4	28.5	34.9
PU 1.1	80.5	7.7	6.1	28.5	34.6
PU 1.2	81.3	6.5	5.7	28.6	34.3
PU 1.3	90.9	6.9	2.4	28.6	30.9
PU 1.4	93.9	6.6	1.6	28.6	30.2
PU 1.5	96.3	6.5	1.1	28.6	29.7

the polyurethane system promotes its thermal stability, which can be evidenced from the increased activation energy values.

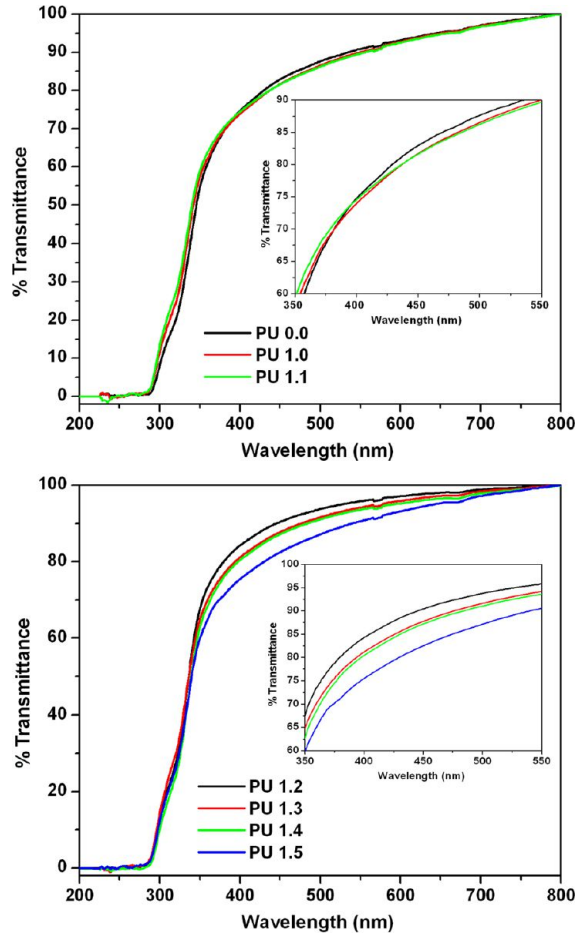

Figure 9. UV−vis spectra for the polyurethane/siloxane films.

DSC and their data for the prepared polyurethane/siloxane films were given in Figure 7 and Table 7. The glass transition temperature (T_g) for the soft segment of control castor oil polyurethane (PU 0.0) is −33.3 °C, and the melting temperature (T_m) for the hard segment is 209.6 °C. The T_g values for the soft segment are increased with increasing silane ratio. This indicates that the increase in cross-linking influences the T_g value of the amorphous phase.[23] The T_g value for the polyurethane/siloxane cross-linked film having higher siloxane content is −27.5 °C (PU 1.5). Similarly, the melting temperature (T_m) of the hard segment increased with respect to the silane ratio. The T_m value for PU 0.0 is 209.6 °C, whereas in the case of polyurethane/siloxane cross-linked structures it is 258.7 °C (PU 1.5). The melting temperature of

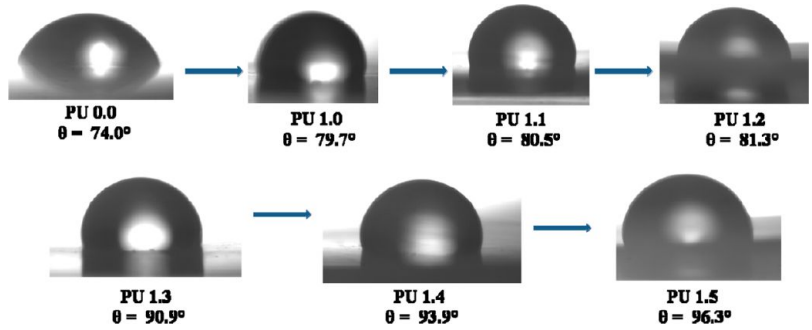

Figure 8. Water droplet on the surface of polyurethane/siloxane films.

dx.doi.org/10.1021/jp3097346 | J. Phys. Chem. B 2013, 117, 2682−2694

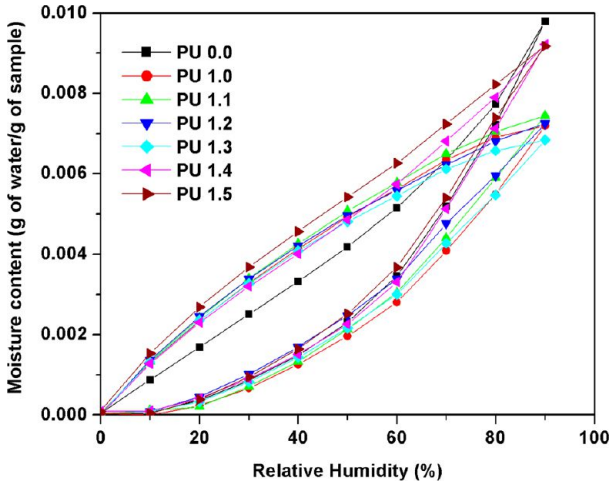

Figure 10. Moisture sorption/desorption isotherm plots for the prepared films.

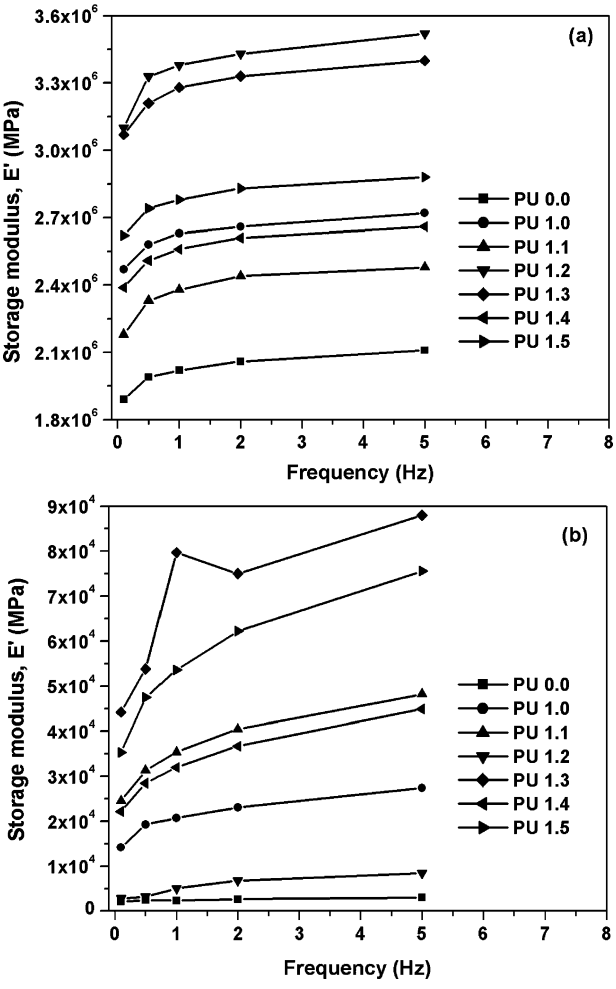

Figure 11. Multifrequency dynamic mechanical analysis for the storage modulus (E') of the polyurethane/siloxane films: (a) −100 and (b) 100 °C.

the polyurethane/siloxane films increases with increasing silane content containing higher siloxane chain in the polyurethane matrix. The cross-linking has a similar effect on the values of melting enthalpies (Table 7).

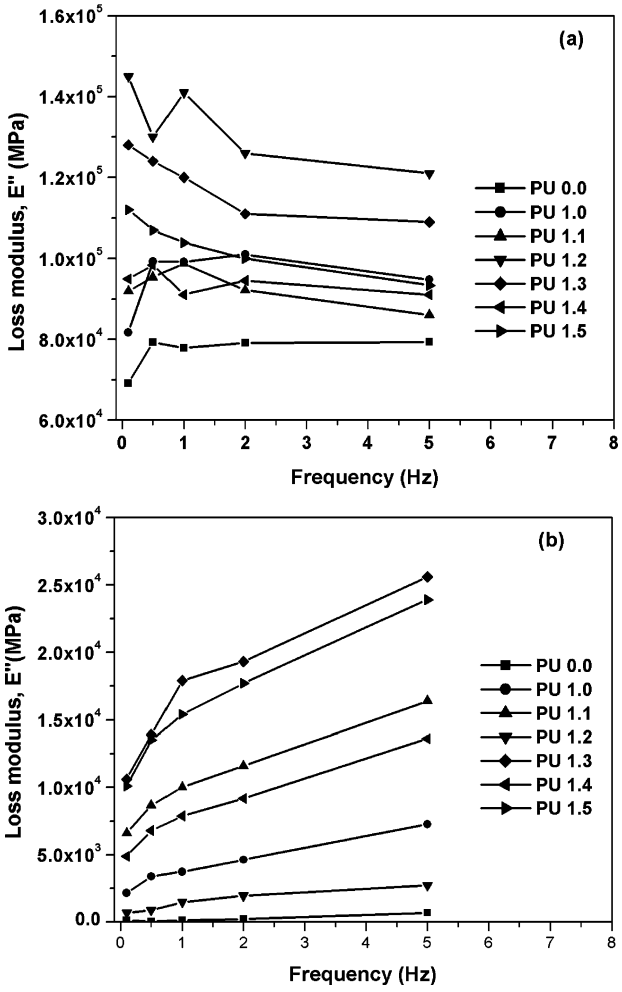

Figure 12. Multifrequency dynamic mechanical analysis for the loss modulus (E'') of the polyurethane/siloxane films: (a) −100 °C and (b) 100 °C.

The hydrophobicity of the polyurethane/siloxane cross-linked films was investigated by measuring the static contact angle. The surface free energy was also calculated from contact angle values using the following Owens and Wendt equation:[50]

$$\gamma_L(1 + \cos\theta) = 2(\gamma_S^d \gamma_L^d)^{1/2} + 2(\gamma_S^p \gamma_L^p)^{1/2} \quad (2)$$

where γ_L = surface tension of the liquids, γ_L^p and γ_L^d = polar and dispersion components of the liquids, and γ_S^p and γ_S^d = polar and dispersion components of the solids.

The static contact angle and surface free energy values were given in Table 8. Contact angle values for the prepared films were increased with increasing silane ratio (Figure 8), and the overall surface energy decreased. The introduction of Si−O−Si network structure to the castor oil polyurethane film increases the contact angle from 74.0 (PU 0.0) to 96.3° (PU 1.5), which indicates a water-repellant surface. Accordingly, the total surface energy decreases from 37.6 (PU 0.0) to 29.7 mJ/m^2 (PU 1.5). The increase in cross-linking of Si−O−Si network structure in the polyurethane matrix plays a vital role in decreasing the surface energy. Usually, siloxanes stratify the surface during the film formation and cross-linking, which reduces the surface energy.[51] The introduction of a siloxane unit changes the surface roughness, which influences the contact angle and surface energy values. The presence of a small amount of

dx.doi.org/10.1021/jp3097346 | J. Phys. Chem. B 2013, 117, 2682−2694

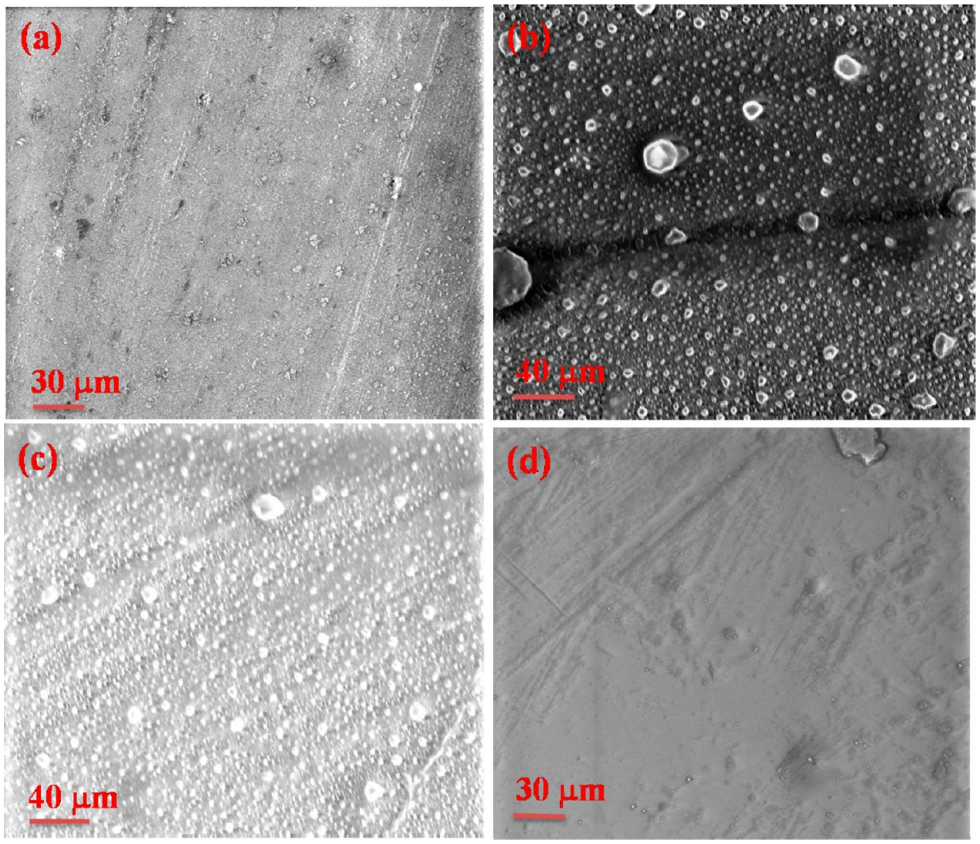

Figure 13. SEM micrographs of the prepared polyurethane/siloxane films: (a) PU 0.0, (b) PU 1.0, (c) PU 1.1, and (d) PU 1.2 (1500×).

siloxane provides a thermodynamic driving force for migration to the material, thereby covering and rendering the surface hydrophobic.[52,53] The wettability of the polyurethane surface was decreased, i.e., hydrophobicity increased with increasing siloxane content (see Table S1 and Figure S1, Supporting Information, for more contact angle images and data). The contact angle values reported were the average of five measurements taken at five different locations of film surface, which proves the homogeneity of the surface.

The optical properties of the prepared polyurethane/siloxane films were investigated using UV−vis spectroscopy and the spectra given in Figure 9. The spectra show that all the film samples have strong absorbance in the range 200−300 nm but are transparent in the region 300−800 nm. The transmittance was almost similar with increasing silane ratio from 0.0 to 1.1. In the case of PU 1.2, it shows higher transmittance up to 90% at a wavelength of 450 nm. After that, the trend is slightly decreased and almost the same for PU 1.3 and PU 1.4. The transmittance of PU 1.5 is similar to the control PU film (PU 0.0). This shows that the silane ratio of 1.2 gives good optical transmittance to the films. Overall, all the samples show good optical transmittance in the visible region. The presence of a siloxane unit could improve the optical transmittance of the polyurethane films. Such transparent PU materials may have applications in lens coatings and optical fiber, etc.[22]

The moisture sorption capacity of the film samples was determined using moisture sorption isotherm analysis. Figure 10 shows the moisture sorption/desorption isotherm plot at 25 °C for the prepared polyurethane/siloxane films. As can be seen from isotherm curves, the water uptake of all the polyurethane films was comparatively less. The shape of the isotherm curve shows a type III isotherm, which is the characteristic feature of hydrophobic or low hydrophilic materials.[54] Only bound water can be physically adsorbed on the surface of the films. The moisture sorption capacity of control PU films (PU 0.0) was high compared to that of the siloxane cross-linked structures. The moisture content of the PU 0.0 film is 0.0098 (g of water/g of sample), which can be explained by the presence of free hydroxyl and isocyanate groups. This determines its slightly hydrophilic character. However, in the case of siloxane cross-linked films, the cross-linking decreases with a decrease in the number of free hydroxyl and isocyanate groups. The introduction of siloxane increases the hydrophobicity in the PU matrix; as a result, the moisture absorption capacity was decreased.[55] The increased hydrophobicity was already proved by the contact angle measurements, which shows a higher contact angle and low surface free energy (Table 8).

The storage modulus (E') and loss modulus (E'') as a function of multiple frequencies (0.1, 0.5, 1, 2, and 5 Hz) at two different temperatures (−100 and 100 °C) were given in Figures 11 and 12. The storage modulus for the polyurethane/siloxane films increases as the silane ratio increases. The E' value provides information about the stiffness, cure, and cross-linking of the polymer films. The cross-linking of a siloxane unit with a polyurethane matrix increases, which increases the E' value of the film samples. This shows that the increasing siloxane content gives mechanical reinforcement to the polyurethane films.[47] The siloxane cross-linking increases the rigidity of the polyurethane matrix, thereby increasing the E' value of the prepared cross-linked film structures.[56] The increment in the E' value was observed at low temperature (−100 °C) as well as high temperature (100 °C). A similar kind of increment in E' value was reported by Ghosh et al.[57] for the polymer−clay nanocomposite system (clay consists of silica

dx.doi.org/10.1021/jp3097346 | J. Phys. Chem. B 2013, 117, 2682−2694

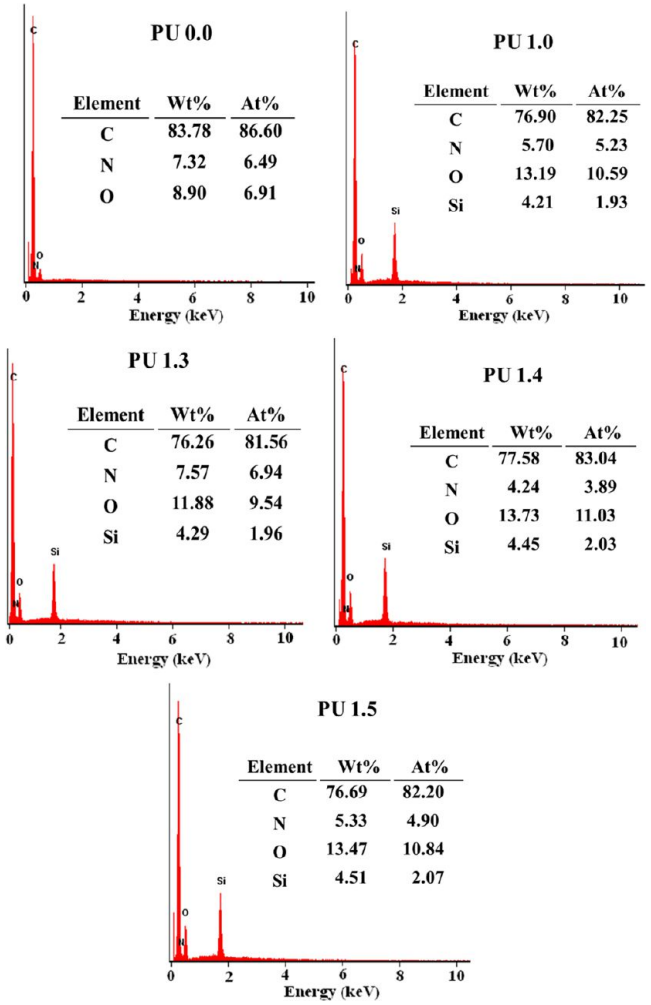

Figure 14. EDX profile of castor oil polyurethane/siloxane films.

layers). The increase of clay loading imparts mechanical reinforcement due to its large surface area, nanosize, and high aspect ratio.[47] From Figure 11, the E' values of the film samples increase as the frequency increases. The increase of storage modulus is high in the case of the lower frequency region, whereas, in the case of the higher frequency region, the above E' increase is relatively small. Thus, the elastic behavior of the film increases as the frequency increases and the storage modulus moves toward higher frequency.[58]

As shown in Figure 12, the loss modulus values increase as the frequency increases. The loss modulus is the measure of energy dissipated under the material stressed. The E'' value at −100 °C was high at low frequency, whereas at higher frequency it decreased. However, at higher temperature (100 °C), the above trend is reversed; i.e., the E'' value increases with increasing frequency. The increase in siloxane unit increases the cross-linking, which gives a better interaction with the polymer matrix. This kind of interaction helps in improving the loss modulus of the film samples, thereby effectively transmitting the stress applied.[59]

Scanning electron microscopy images of the prepared films are displayed in Figure 13. In the case of the PU 0.0 sample, the surface was uniform. As the amount of silane ratio increases, the cross-linking also increases. This changes the surface with the phase separated one (PU 1.0). This could be explained by the fact that the siloxane blocks were microphase separated.[60] The

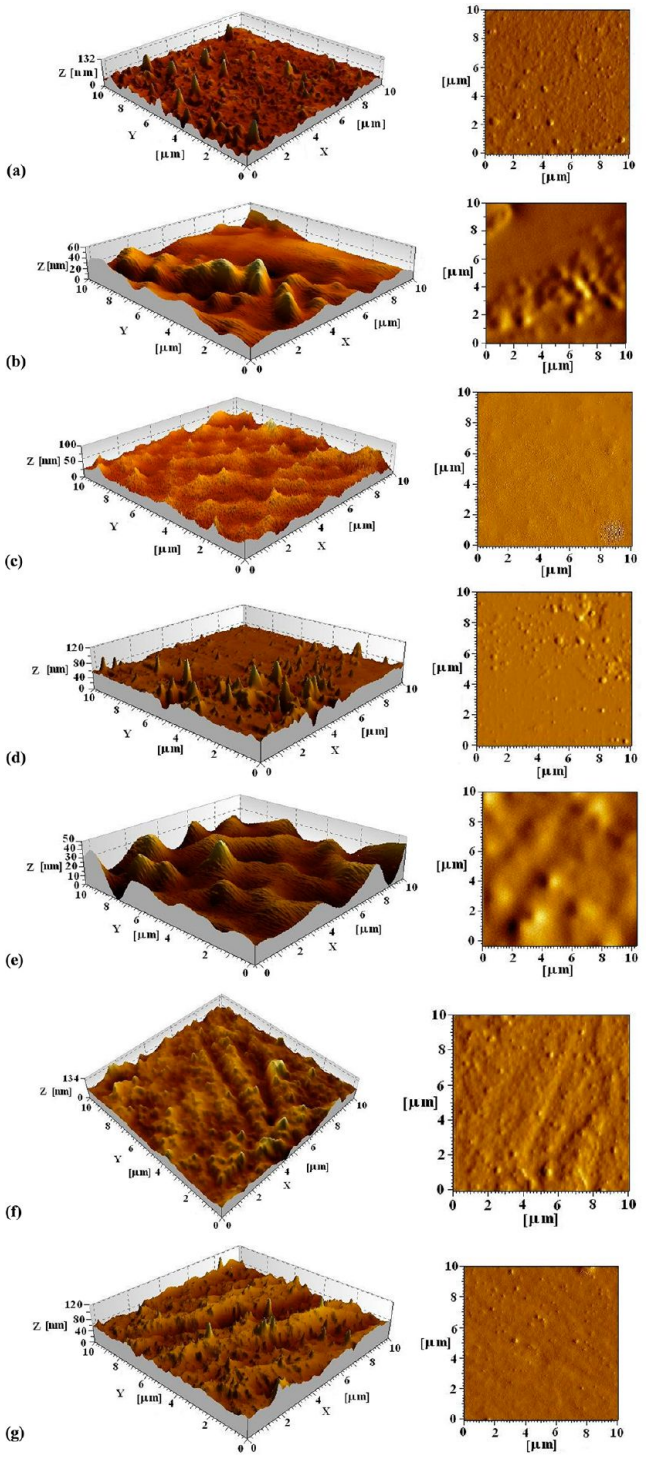

Figure 15. AFM images of the polyurethane/siloxane films: (a) PU 0.0 (scale: 0−1.25 nm), (b) PU 1.0 (scale: 0−0.185 nm), (c) PU 1.1 (scale: 0−1.85 nm), (d) PU 1.2 (scale: 0−0.975 nm), (e) PU 1.3 (scale: 0−0.135 nm), (f) PU 1.4 (scale: 0−0.825 nm), and (g) PU 1.5 (scale: 0−1.1 nm) (scale for right side image).

incorporation of siloxane shows some microdomains in the case of cross-linked film structures (Figure 13b). These microdomains mainly arise from the polysiloxane unit.[61]

Figure 14 shows the EDX profile of the prepared polyurethane/siloxane films. In the case of PU 0.0, all the expected elements (C, N, and O) were present. However, in the cases of siloxane incorporated PUs, the characteristic Si

dx.doi.org/10.1021/jp3097346 | J. Phys. Chem. B 2013, 117, 2682−2694

atom also present including C, N, and O. The element Si percentage was increased with increasing silane ratio (4.21 and 4.51% for PU 1.0 and PU 1.5, respectively). This shows that increasing the cross-linking agent ratio increases the Si percentage in the whole mass of the sample. The EDX profile confirms the presence of expected atoms in the polyurethane sample.

The surface morphology of the castor oil polyurethane/siloxane cross-linked films was examined using AFM. Figure 15 shows AFM images of the polyurethane/siloxane films taken in tapping mode. The surface roughness of the film structure changes with increasing silane ratio, which means that the increasing siloxane cross-linking imparts smoothness to the film structures. The sample PU 0.0 (Figure 15a) had a surface of irregularity with heights and the root-mean-square (RMS) surface roughness value (R_q) of 13.4 nm. AFM images show the smooth surface obtained for the siloxane cross-linked structures. In the case of cross-linked film structures, some discontinuous regions with relatively bright and dark parts were observed (Figure 15b). This implies the existence of microphase separation in the film structures. However, increasing the silane content shows a more distinct microphase separated structure, which gives a smoothed surface. The RMS roughness value for the PU 1.5 is 4.7 nm. The increasing siloxane cross-linking had a different surface structure with a smaller node of 0.15 μm observed (PU 1.5).

The surface roughness is the important factor for the wettability of the surface.[62] The roughness values (R_q) for the PU 0.0 and PU 1.5 samples are 13.4 and 4.7 nm, respectively. Accordingly, the surface free energies are 37.6 and 29.7 mJ/m^2 for PU 0.0 and PU 1.5, respectively. A similar kind of decreasing surface energy values (i.e., increasing contact angle values) for the silane treated titanium surfaces was reported by Matinlinna et al.[63] The silane during treatment forms a siloxane network structure on the surface of the titanium, which gives hydrophobicity to the films. The surface roughness of the film decreases as the siloxane cross-linking increases, which affects the wettability of the films. The contact angle also increases with decreasing RMS surface roughness value. The decreased surface roughness imparts reduced wettability to the film structures.[64] An et al.[65] observed that the covering of the cellulose substrate surface by polysiloxane resulted in reducing the roughness of the surface. Furthermore, the contact angle of the surface is greater than 90°, indicating the hydrophobicity of the surface. In our case, increasing the siloxane cross-linking imparts hydrophobicity to the films, which means the surface was covered with more siloxane groups. This is the main cause for the reduced wettability of the surface (reduce in surface roughness).

4. CONCLUSIONS

Castor oil based polyurethane/siloxane cross-linked structure films were prepared through a sol−gel process. In the first step, castor oil polyurethane prepolymer was made from castor oil and isophorone diisocyanate using dibutyltin dilaurate catalyst in chloroform. In the second step, 3-aminopropyl trimethoxysilane was introduced in the system, which forms a urea linkage with the polyurethane prepolymer. Furthermore, the siloxane unit was formed through a hydrolysis and condensation process of the methoxy group present in the silane moiety. The formation of cross-linked structure was confirmed from ATR-FTIR spectroscopy. ^{29}Si solid state NMR gives the respective chemical shift of Q^3 and T^3 environment present in polyurethane/siloxane films, thereby giving evidence for the formation of siloxane network structure. TGA studies show that increasing siloxane cross-linking increases the thermal stability of the resultant films, which is evidenced from activation energy values. Contact angle studies show that the surface free energy decreased from 37.6 to 29.7 mJ/m^2 for PU 0.0 and PU 1.5, respectively. This shows that increasing silane ratio, i.e., cross-linking, increased the hydrophobicity of the film. The moisture sorption capacity of the films decreased with increasing siloxane content. SEM images show that the incorporation of siloxane gives microdomains, which are mainly from the polysiloxane unit. AFM revealed that the higher level of siloxane cross-linking decreased the surface roughness value. The decreased surface roughness value shows that the surface roughness imparts a reducing wettability to the films.

■ ASSOCIATED CONTENT

Supporting Information

Table S1 (water contact angle values of polyurethane/siloxane films at four different places), Figure S1 (image of a water droplet on polyurethane/siloxane films at four different places). This material is available free of charge via the Internet at http://pubs.acs.org.

■ AUTHOR INFORMATION

Corresponding Author

*E-mail: abmandal@hotmail.com; abmandal@clri.res.in. Phone: +91 44 24910846/0897. Fax: +91 44 24912150.

Notes

The authors declare no competing financial interest.

■ ACKNOWLEDGMENTS

One of the authors (K.M.S.M.) acknowledges CSIR, India (grant number 31/6(362)/2012-EMR-I) for Senior Research Fellowship. We are grateful to Dr. Vijayamohanan K. Pillai and Dr. R. H. Suresh Bapu, CECRI, Karaikudi, for permitting to perform AFM analysis and also we would to like thank Mr. Rathish Kumar and Mrs. Bhagyalakshmi, CECRI, Karaikudi, for helping with the AFM analysis. We thank Mr. S. Radhakrishnan, CECRI, Karaikudi, for assisting with the ^{29}Si solid state CP/MAS NMR analysis. The authors wish to thank Dr. K. Ravichandiran, Dr. B. T. N. Sridhar, Mr. Palanikumar, and Mrs. Uma, MIT, Chennai, for permitting and helping us to take DMA analysis. We also thank Mr. Johnsy George, DFRL, Mysore, for helping with the Moisture sorption analysis. The authors wish to thank Dr. Aruna Dhathathreyan and Mrs. Kamatchi, CLRI, for providing support to contact angle measurements. We thank Dr. Debasis Samanta, CLRI, for valuable discussions and Ms. Jaya Paul for assistance.

■ REFERENCES

(1) Gurusamy-Thangavelu, S. A.; Emond, S. J.; Kulshrestha, A.; Hillmyer, M. A.; Macosko, C. W.; Tolman, W. B.; Hoye, T. R. *Polym. Chem.* **2012**, *3*, 2941−2948.

(2) Xia, Y.; Larock, R. C. *Macromol. Rapid Commun.* **2011**, *32*, 1331−1337.

(3) Jaisankar, S. N.; Lakshminarayana, Y.; Radhakrishnan, G.; Ramasami, T. *Polym.-Plast. Technol. Eng.* **1996**, *35*, 781−789.

(4) Sharma, V.; Kundu, P. P. *Prog. Polym. Sci.* **2008**, *33*, 1199−1215.

(5) Amado, F. D. R.; Rodrigues, L. F., Jr.; Forte, M. M. C.; Ferreira, C. A. *Polym. Eng. Sci.* **2006**, *46*, 1485−1489.

(6) Jaisankar, S. N.; Murali Sankar, R.; Seeni Meera, K.; Mandal, A. B. *Soft Mater.* **2013**, *11*, 55−60.

(7) Liu, D.; Tian, H.; Zhang, L.; Chang, P. R. *Ind. Eng. Chem. Res.* **2008**, *47*, 9330−9336.
(8) Murali Sankar, R.; Seeni Meera, K.; Mandal, A. B.; Jaisankar, S. N. *High Perform. Polym.* **2013**, *25*, 135−145.
(9) Kyung Lee, S.; Ho Yoon, S.; Chung, I.; Hartwig, A.; Kyu Kim, B. *J. Polym. Sci., Part A: Polym. Chem.* **2011**, *49*, 634−641.
(10) Jaisankar, S. N.; Nelson, D. J.; Brammer, C. N. *Polymer* **2009**, *50*, 4775−4780.
(11) Mishra, A.; Das Purkayastha, B. P.; Roy, J. K.; Aswal, V. K.; Maiti, P. *J. Phys. Chem. C* **2012**, *116*, 2260−2270.
(12) Dong, Z.; Li, Y.; Zou, Q. *Appl. Surf. Sci.* **2009**, *255*, 6087−6091.
(13) Hu, Y. S.; Tao, Y.; Hu, C. P. *Biomacromolecules* **2001**, *2*, 80−84.
(14) Piccin, E.; Coltro, W. K. T.; Fracassi da Silva, J. A.; Neto, S. C.; Mazo, L. H.; Carrilho, E. *J. Chromatogr., A* **2007**, *1173*, 151−158.
(15) Jaisankar, S. N.; Sathya, R.; Hariharan, S.; Mohan, R.; Saravanan, P.; Samanta, D.; Mandal, A. B. *Ind. Eng. Chem. Res.* **2013**, *52*, 1379−1387.
(16) Hu, Y.; Samanta, D.; Parelkar, S. S.; Hong, S. W.; Wang, Q.; Russell, T. P.; Emrick, T. *Adv. Funct. Mater.* **2010**, *20*, 3603−3612.
(17) Ghosh, S.; Maity, S.; Jana, T. *J. Mater. Chem.* **2011**, *21*, 14897−14906.
(18) Seeni Meera, K. M.; Murali Sankar, R.; Murali, A.; Jaisankar, S. N.; Mandal, A. B. *Colloids Surf., B* **2012**, *90*, 204−210.
(19) Dahmouche, K.; Santilli, C. V.; Pulcinelli, S. H. *J. Phys. Chem. B* **1999**, *103*, 4937−4942.
(20) Sanchez, C.; Julian, B.; Belleville, P.; Popall, M. *J. Mater. Chem.* **2005**, *15*, 3559−3592.
(21) Lambert, J. B.; Gurusamy-Thangavelu, S. A.; Ma, K. *Science* **2010**, *327*, 984−986.
(22) Tan, H.; Yang, D.; Xiao, M.; Han, J.; Nie, J. *J. Appl. Polym. Sci.* **2009**, *111*, 1936−1941.
(23) Sen, P.; Mukherjee, S.; Patra, A.; Bhattacharyya, K. *J. Phys. Chem. B* **2005**, *109*, 3319−3323.
(24) Arunbabu, D.; Shahsavan, H.; Zhang, W.; Zhao, B. *J. Phys. Chem. B* **2013**, *117*, 441−449.
(25) Subramani, S.; Lee, J. M.; Cheong, I. W.; Kim, J. H. *J. Appl. Polym. Sci.* **2005**, *98*, 620−631.
(26) Alexandru, M.; Cazacu, M.; Cristea, M.; Nistor, A.; Grigoras, C.; Simionescu, B. C. *J. Polym. Sci., Part A: Polym. Chem.* **2011**, *49*, 1708−1718.
(27) Adhikari, R.; Gunatillake, P. A.; McCarthy, S. J.; Bown, M.; Meijs, G. F. *J. Appl. Polym. Sci.* **2003**, *87*, 1092−1100.
(28) Rivero, P. J.; Urrutia, A.; Goicoechea, J.; Zamarreno, C. R.; Arregui, F. J.; Matias, I. R. *Nanoscale Res. Lett.* **2011**, *6*, 305−311.
(29) Choi, T.; Masser, K. A.; Moore, E.; Weksler, J.; Padsalgikar, A.; Runt, J. *J. Polym. Sci., Part B: Polym. Phys.* **2011**, *49*, 865−872.
(30) Rhodes, N. P.; Bellon, J. M.; Juliabujan, M.; Soldani, G.; Hunt, J. A. *J. Mater. Sci. Mater. Med.* **2005**, *16*, 1207−1211.
(31) Ni, H.; Johnson, A. H.; Soucek, M. D.; Grant, J. T.; Vreugdenhil, A. J. *Macromol. Mater. Eng.* **2002**, *287*, 470−479.
(32) Pieper, R. J.; Ekin, A.; Webster, D. C.; Casse, F.; Callow, J. A.; Callow, M. E. *J. Coat. Technol. Res.* **2007**, *4*, 453−461.
(33) Sommer, S. A.; Byrom, J. R.; Fischer, H. D.; Bodkhe, R. B.; Stafslien, S. J.; Daniels, J.; Yehle, C.; Webster, D. C. *J. Coat. Technol. Res.* **2011**, *8*, 661−670.
(34) Wu, Z.; Tong, W.; Jiang, W.; Liu, X.; Wang, Y.; Chen, H. *Colloids Surf., B* **2012**, *96*, 37−43.
(35) Mishra, A. K.; Chattopadhyay, D. K.; Sreedhar, B.; Raju, K. V. S. N. *Prog. Org. Coat.* **2006**, *55*, 231−243.
(36) Meera, K. M. S.; Sankar, R. M.; Jaisankar, S. N.; Mandal, A. B. *Colloids Surf., B* **2011**, *86*, 292−297.
(37) Xia, Y.; Larock, R. C. *Polymer* **2010**, *51*, 2508−2514.
(38) Martinelli, M.; Luca, M. A.; Bechi, D. M.; Mitidieri, S. *J. Sol-Gel Sci. Technol.* **2009**, *52*, 202−209.
(39) Karak, N.; Rana, S.; Cho, J. W. *J. Appl. Polym. Sci.* **2009**, *112*, 736−743.
(40) Prabhakar, A.; Chattopadhyay, D. K.; Jagadeesh, B.; Raju, K. V. S. N. *J. Polym. Sci., Part A: Polym. Chem.* **2005**, *43*, 1196−1209.
(41) Chiang, C.-L.; Ma, C-C. M. *Eur. Polym. J.* **2002**, *38*, 2219−2224.
(42) Radi, B.; Wellard, R. M.; George, G. A. *Macromolecules* **2010**, *43*, 9957−9963.
(43) Brus, J.; Spirkova, M.; Hlavata, D.; Strachota, D. *Macromolecules* **2004**, *37*, 1346−1357.
(44) Wencel, D.; Barczak, M.; Borowskic, P.; McDonagh, C. *J. Mater. Chem.* **2012**, *22*, 11720−11729.
(45) Petrovic, Z. S.; Yang, L. T.; Zlatanic, A.; Zhang, W.; Javni, I. *J. Appl. Polym. Sci.* **2007**, *105*, 2717−2727.
(46) Kumar, M. N. S.; Siddaramaiah.. *J. Appl. Polym. Sci.* **2007**, *106*, 3521−3528.
(47) Turhan, Y.; Dogan, M.; Alkan, M. *Ind. Eng. Chem. Res.* **2010**, *49*, 1503−1513.
(48) Chiang, C.-L.; Chang, R.-C.; Chiu, Y.-C. *Thermochim. Acta* **2007**, *453*, 97−104.
(49) Tomasic, V.; Brnardic, I.; Jenei, H.; Kosar, V.; Zrncevic, S. *Chem. Biochem. Eng. Q.* **2011**, *25*, 283−287.
(50) Owens, D. K.; Wendt, R. C. *J. Appl. Polym. Sci.* **1969**, *13*, 1741−1747.
(51) Bai, C.; Zhang, X.; Dai, J.; Wang, J. *J. Coat. Technol. Res.* **2008**, *5*, 251−257.
(52) Stiubianu, G.; Nicolescu, A.; Nistor, A.; Cazacu, M.; Varganici, C.; Simionescu, B. C. *Polym. Int.* **2012**, *61*, 1115−1126.
(53) Kulkarni, S. A.; Ogale, S. B.; Vijayamohanan, K. P. *J. Colloid Interface Sci.* **2008**, *318*, 372−379.
(54) Ng, E. P.; Mintova, S. *Microporous Mesoporous Mater.* **2008**, *114*, 1−26.
(55) Stiubianu, G.; Racles, C.; Nistor, A.; Cazacu, M.; Simionescu, B. C. *Cellulose Chem. Technol.* **2011**, *45*, 157−162.
(56) Tsai, M. H.; Chiang, P. C.; Whang, W. T.; Ko, C. J.; Huang, S. L. *Surf. Coat. Technol.* **2006**, *200*, 3297−3302.
(57) Ghosh, S.; Sannigrahi, A.; Maity, S.; Jana, T. *J. Phys. Chem. C* **2011**, *115*, 11474−11483.
(58) Menard, K. P. Dynamic Mechanical Analysis. *A Practical Introduction*; CRC Press: Boca Raton, FL, 1999.
(59) Tannenbaum, R.; King, S.; Lecy, J.; Tirrell, M.; Potts, L. *Langmuir* **2004**, *20*, 4507−4514.
(60) Zhu, X. L.; Jiang, X. B.; Zhang, Z. G.; Kong, X. Z. *Chin. J. Polym. Sci.* **2011**, *29*, 259−266.
(61) Li, C. Y.; Chen, J. H.; Chien, P. C.; Chiu, W. Y.; Chen, R. S.; Don, T. M. *Polym. Eng. Sci.* **2007**, *47*, 625−632.
(62) Kostov, K. G.; Dos Santos, A. L. R.; Nascente, P. A. P.; Kayama, M. E.; Mota, R. P.; Algatti, M. A. *J. Appl. Polym. Sci.* **2012**, *125*, 4121−4127.
(63) Matinlinna, J. P.; Areva, S.; Lassila, L. V. J.; Vallittu, P. K. *Surf. Interface Anal.* **2004**, *36*, 1314−1322.
(64) Pandiyaraj, K. N.; Selvarajan, V.; Deshmukh, R. R.; Gao, C. *Vacuum* **2009**, *83*, 332−339.
(65) An, Q.; Wang, Q.; Li, L.; Huang, L. *Text. Res. J.* **2009**, *79*, 89−93.